Coarse-Grained Transmembrane Proteins: Hydrophobic Matching, Aggregation, and Their Effect on Fusion

A. F. Smeijers,* K. Pieterse, A. J. Markvoort, and P. A. J. Hilbers

Department of Biomedical Engineering, Technische Universiteit Eindhoven, P.O. Box 513, 5600 MB Eindhoven, The Netherlands

Received: March 31, 2006

Molecular transport between organelles is predominantly governed by vesicle fission and fusion. Unlike experimental vesicles, the fused vesicles in molecular dynamics simulations do not become spherical readily, because the lipid and water distribution is inappropriate for the fused state and spontaneous amendment is slow. Here, we study the hypothesis that enhanced transport across the membrane of water, lipids, or both is required to produce spherical vesicles. This is done by adding several kinds of model proteins to fusing vesicles. The results show that equilibration of both water and lipid content is a requirement for spherical vesicles. In addition, the effect of these transmembrane proteins is studied in bilayers and vesicles, including investigations into hydrophobic matching and aggregation. Our simulations show that the level of aggregation does not only depend on hydrophobic mismatch, but also on protein shape. Additionally, one of the proteins promotes fusion by inducing pore formation. Incorporation of these proteins allows even flat membranes to fuse spontaneously. Moreover, we encountered a novel spontaneous vesicle enlargement mechanism we call the engulfing lobe, which may explain how lipids added to a vesicle solution are quickly incorporated into the inner monolayer.

1. Introduction

The principal function of cell membranes is compartmentalization: each cellular process must be carried out in a specific environment, in a controlled way. For this to function properly, the appropriate molecules must be transported between the various compartments or organelles. Vesicular trafficking is utilized in directed transport; the vesicles fuse with the appropriate target organelle, releasing their contents inside. With molecular dynamics (MD) simulations, processes at the nanoscale can be studied in detail. As simulating the complete fusion pathway is computationally unfeasible using fully atomistic MD, often a coarse-grained approach is used.[1−3]

A vesicle's shape is preferentially spherical so it has minimal membrane tension distributed uniformly over the surface. Whereas the coarse-grained MD vesicle fusion simulations display the proper fusion processes, the resultant vesicles remain tubular instead of becoming spherical as they do experimentally, the reason being that during fusion the total water content and lipid distribution over the bilayers does not change markedly. Hence, the fused vesicle's volume is too small as compared to its membrane area, and its lipid distribution is not adapted to the new situation. In addition, the membrane's capacity for water transport and lipid flip-flop is low as compared to the required transport and, more importantly, the accessible simulation time. We hypothesize that, to promote fused vesicles to become spherical, increased water transport, increased lipid flip-flop, or both is needed. To this end, we incorporate functional transmembrane proteins into our lipid membranes. To increase the water permeability, we have reproduced the water channel function of aquaporin. To increase the rate of lipid flip-flop, we built two scramblase proteins: one being a bare transmembrane helix, which is supposed to induce flip-flop;[4] the other a prototype of the class of pore-forming antimicrobial peptides, which is reported to form pores and promote flip-flop.[5] Aside from fused vesicles becoming spherical or not, the incorporation of coarse-grained proteins presents challenges of its own. The requirements of coarse-grained proteins need to be elucidated. Is it even possible to build authentic transmembrane proteins with a coarse-grained model? The proteins need not only perform their desired function, but also exhibit realistic interactions with the membrane and other proteins. Does the membrane adapt to the transmembrane protein, as the hydrophobic matching theory suggests, and do the proteins aggregate when multiple proteins are incorporated in a membrane?

In addition to the effects of the proteins on the vesicles following fusion, they may also have an effect during the initial stages of fusion. In particular, one of the scramblases possesses characteristics displayed by the putative proteinaceous fusion pore model;[6] does such a protein indeed promote fusion?

In this paper, we investigate these questions by using our coarse-grained lipid model for proteins.[7] However, despite focusing on proteins, we also encountered a novel spontaneous vesicle enlargement mechanism, which functions without protein involvement. This mechanism may explain how lipids added to a solution of vesicles get incorporated into the inner monolayers of these vesicles.

2. Methods

2.1. Model. *2.1.1. Lipid, Water, and Force Field.* The coarse-grained model for lipid and water has been presented in a previous paper.[7] The lipid is modeled by four hydrophilic H particles, and two tails of four hydrophobic T particles each (Figure 1a). It is based on the glycerophospholipid class of which dipalmitoylphosphatidylcholine (DPPC) is a prime example. Water particles are denoted by W. All bonds are regulated by

* Corresponding author. E-mail: a.f.smeijers@tue.nl.

10.1021/jp062012y CCC: $33.50
Published on Web 06/20/2006

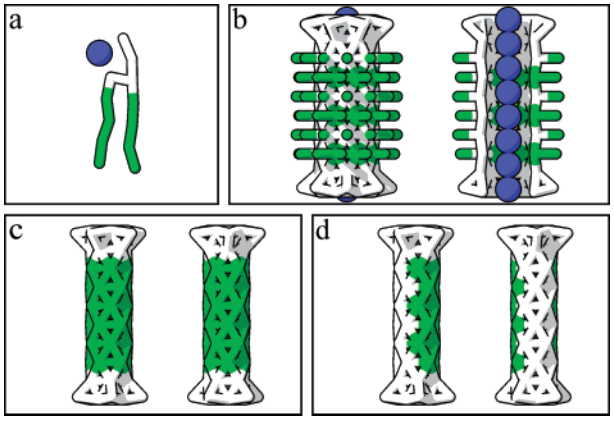

Figure 1. The coarse-grained water, lipid, and proteins. (a) Stick representation of the coarse-grained lipid molecule with hydrophilic headgroups (white) and hydrophobic tails (green) and a van der Waals representation of the water particle (blue). (b) Stick representation of the coarse-grained water channel showing its structure and a cross-section highlighting the hydrophilic band and rings inside the channel. (c) Front and side view of the type A scramblase; it has a purely hydrophobic transmembrane part. (d) Front and side view of the type B scramblase; it has a hydrophilic band down its side.

harmonic bond potentials; the nonbonded interactions are governed by truncated shifted Lennard-Jones potentials. The model was fitted for water and alkanes, instead of lipids in a bilayer, so there is no unnatural bias toward membrane formation. To ensure flexibility of our lipids and to be able to investigate vesicle fusion by using relatively small unstressed vesicles, no bending potentials are applied.

Because of the smooth potentials and lack of hydrogen-bond network, the diffusional time scales of coarse-grained MD simulations are not identical to the time scale implied. One could decide on a calibration factor to make, for instance, the lateral lipid diffusion a perfect fit. However, in the same system other diffusion coefficients require a different calibration factor, as the factor varies with the mass and size of the particles.[8] Because a general calibration factor for a mixed system does not exist, we have chosen to present the time-dependent results without such a factor.

2.1.2. Water Channel. In the present study, we extend this coarse-grained model with two proteins, the first being a water channel to enhance water transport through bilayers. To keep our model as simple as possible, we only use existing H and T particles and the previously mentioned potentials. The challenges we are presented with are as follows: is it possible to compose a coarse-grained water channel, and what requirements must such a channel adhere to? We base our design on the protein aquaporin.

In nature, when active in a membrane, aquaporin functions as a passive water channel. Its four subunits each make up a narrow pore. Two funnel-shaped apertures lead to the pore, formed by the tilted arrangement of seven helical structures. The channel apertures have series of accessible carbonyl oxygens forming hydrophilic paths leading to the pore. The pore is largely hydrophobic with discrete hydrophilic spots that provide an alternative for the hydration shell of water. The pore lining facilitates fast water transport.[9,10]

The coarse-grained water channel is built resembling one aquaporin subunit. An ideal channel is stable in a lipid membrane, stays open most of the time, and provides rapid water transport. However, the simplicity of the underlying model directs the design, as only H and T particles are used and the potentials to favor a specific conformation are limited to Lennard-Jones and bond potentials. Therefore, helical structures are impossible to reproduce. Nonetheless, a simple hollow cylinder suffices to represent a pore.

The cylinder is composed of a stack of 10 rings, whereby all particles are bound in a triangular mesh (Figure 1b). The internal ring consists of 8 particles and has an effective diameter of 0.70 nm, whereas the effective diameter of W is 0.52 nm. The pore is wide and flexible enough to occasionally let water particles trade places, just like fully atomistic simulations of aquaporin[11] suggest. To ensure the semi-hydrophilic pore remains stable in the bilayer, it is coated with particles matching the local polarity of the bilayer, just as proteins are in vivo. To avoid any loose ends that would obstruct the pore opening, the pore ends are built as tetrahedrons.

Of various pore lining patterns tested, a pattern resembling the hydrophobicity of the aquaporin interior proved to encourage water flow best. Accordingly, the water channel has hydrophilic apertures, the middle consists of alternating hydrophilic and hydrophobic rings, and a hydrophilic band from top to bottom leads water particles through the pore. An additional advantage of this pattern is that the pore will collapse less easily as mutual repulsion between the hydrophilic and hydrophobic parts prevents complete flattening. Furthermore, the channel is filled from the start such that no time is lost on filling the channel.

Our coarse-grained proteins share similarities with a coarse-grained channel developed by Lopez et al.,[12] which in turn was made to resemble a fully atomistic carbon nanotube.[13] Their protein is a simple hydrophobic cylinder built from a similar mesh either with or without hydrophilic ends. These ends are found to enhance its position in the membrane and reduce occlusion by lipid tails.

2.1.3. Scramblases. Next, we add scramblases to our coarse-grained model. These proteins enhance the flip-flop of lipids. Again, we only use H and T particles and base the design on real proteins.

In lipid bilayers, the structural and amphiphilic properties of phospholipids are such that there is hardly any spontaneous flip-flop. The half-times of spontaneous membrane translocation for in vitro vesicle membranes are in the order of days,[14,15] whereas in eukaryotic plasma membranes flip-flop is in the order of months.[16] In cell membranes, the composition of phospholipids in each face of the bilayer is different and stable; this is associated with cellular processes such as membrane recognition and phospholipid−protein interaction.[16] On the other hand, sometimes lipid flip-flop is asked for in the cell, for example, with apoptosis or in the biogenic membranes, the membranes where lipid and protein synthesis is localized. To maintain the right lipid distribution, or to disrupt it, several protein groups are present in the cell.

In general, there are two classes of proteins promoting flip-flop, flippases that actively maintain an asymmetric lipid distribution of the membrane by transporting specific lipids in one direction and scramblases that passively equilibrate the membrane.[17] Examples of the first class are aminophospholipid translocase and ABC transporters, while phospholipid scramblase is a scramblase.[15,18]

Another scramblase protein is assumed to exist in biogenic membranes. Phospholipids are synthesized exclusively on the cytoplasmic monolayer of the endoplasmic reticulum (ER) in eukaryotes and the plasma membrane in prokaryotes. If not resolved, this would result in unwanted membrane curvature, the lack of which indicates the presence of a scramblase. Its activity has been measured and shown to be passive, bi-directional, headgroup unspecific, partially sensitive to protein

denaturing agents, and satiable.[15,18] Historically, this putative protein was named flippase, but in fact it functions as a scramblase. With half-times of 8−16 s for phosphatidylcholine and phosphatidylethanolamine,[19] it is relatively fast.

Until a flippase protein is indisputably identified in biogenic membranes, the question remains whether there is a single flippase, a group of flippases, or no flippases at all. In the latter case, as advocated by Kol et al.,[4,18,20] flip-flop would be a general property of biogenic membranes resulting from the mere presence of proteins. An intrinsic flip-flop capacity would be advantageous, as newly synthesized lipids would only have to move down their gradient to be evenly distributed over the membrane leaflets. This hypothesis has been tested in various experiments, for example, by using model transmembrane peptides (XALPs) in *E. coli* membrane liposomes. These peptides form helices with a hydrophobic core consisting of alternating alanine and leucine residues. The core is capped with two hydrophilic residues and additional endgroups. With these peptides, half-times were found to increase to the order of minutes at peptide-to-lipid ratios of 1:250.[4] Fractionated protein extracts[21] and transmembrane proteins with a primary function not linked to flip-flop[20] give different flip-flop rates for different proteins, indicating that not all membrane proteins are capable of inducing flip-flop. Two modes of flip-flop were postulated. One is that a transmembrane protein produces a somewhat more hydrophilic environment.[4] The second is that a single transmembrane protein locally disturbs the bilayer with dynamic protein−lipid interactions such as rotational motion, wobbling, tilting, or bending of the helix.[18]

Pore-forming antimicrobial peptides are another kind of flip-flop peptide present in nature. They are α-helical transmembrane peptides with a hydrophilic side covering about 40% of their surface; examples include magainin 2[5] and pandinin 2.[22] They are believed to form pores in the cell membrane, thereby disrupting the transmembrane electrochemical gradient and inhibiting cell growth or even killing the cell.[23] Antimicrobial peptides spark a renewed interest because bacteria become increasingly resistant to conventional antibiotics.

A coarse-grained transmembrane protein has been constructed with the aim of reproducing the fast flippase activity of biogenic membranes and the structure of the XALP model peptides. As its function is fast and indiscriminate flip-flop, our protein is simply called scramblase. The coarse-grained water channel design is used as a basis. Likewise, scramblase is a cylinder measuring 10 rings in height, including tetrahedral hydrophilic caps. The tetrahedral ends remain for their presumed role as shields against water penetrating the membrane. Modifications are the reduced ring size of 5 particles, so the cylinder's core is inaccessible to water particles, and the absence of hydrophobic coating particles (Figure 1c). In the configuration where the core is entirely hydrophobic and the scramblase resembles XALPs, we refer to the protein as a type A scramblase. Type B denotes the configuration in which the scramblase is made similar to pore-forming antimicrobial peptides by giving it a two particle wide hydrophilic band down the side (Figure 1d).

2.2. Simulations. All simulations described in this paper have been performed at constant temperature (307 K) and constant pressure (1 bar) with time steps of 24 fs and using our in-house developed molecular dynamics code PumMa.[7]

Lipid bilayers were made by randomly distributing a number of lipids in a simulation box filled with water particles. When the simulation is run, a bilayer is formed spontaneously. Membranes incorporating transmembrane proteins were constructed in the same manner by adding a transmembrane protein to the random initial state. Pressure scaling was applied independently in all three spatial directions such that no unnatural stress was introduced in the bilayer.

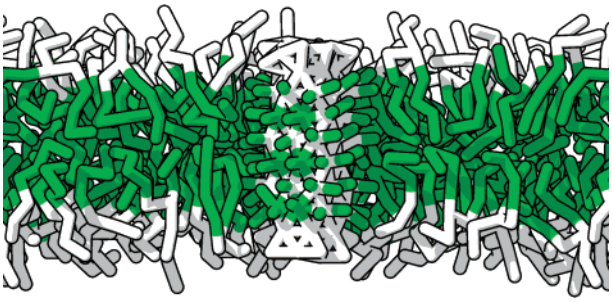

Figure 2. A cross-sectional view through the lipid bilayer showing the position of the water channel. Water is omitted for clarity.

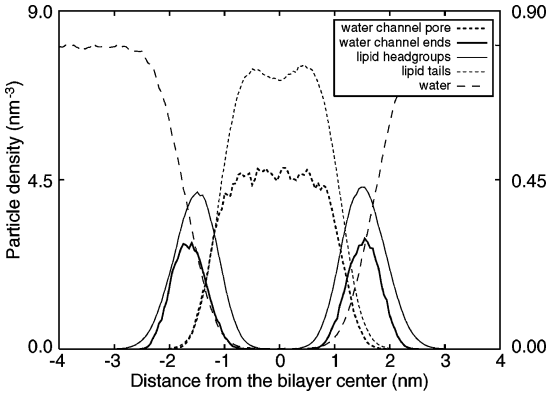

Figure 3. Density profiles of the bilayer (left axis) and the water channel (right axis) superimposed. The difference in values is due to the difference in the amount of lipid and protein particles.

Vesicles were made by moving a bilayer to a larger water-filled simulation box. When the simulation is run, the bilayer curls to minimize its edge, ultimately forming a vesicle.[7]

The setup for the vesicle fusion simulations is made by duplicating the vesicle's simulation box. Both instances are placed next to each other in a larger simulation box, in such a way that the vesicles start at a relatively small distance from each other; on average, 6 layers of water particles remain in between. The parts of the box devoid of particles are again filled with additional water. In contrast to the practice of others,[2,3] no constraints are put on the vesicles during the simulations.

3. Results

3.1. Bilayers. To begin with, the effect of transmembrane protein addition is determined in bilayer systems. First, general effects as hydrophobic matching and aggregation are studied, followed by the proteins' specific transport activities.

3.1.1. Hydrophobic Matching. First, we study the incorporation of a single protein in the bilayer. In a simulation of 144 ns, the water channel remained anchored at the water−lipid interface. The channel seems to fit seamlessly in the bilayer (Figure 2). On the other hand, the peaks in the density profile (Figure 3) show that the channel does not fit perfectly and is somewhat too large. However, shortening the channel by removal of one particle layer would create a larger mismatch. In this simulation, the overall bilayer thickness, as measured by the distance between headgroup density peaks, is on average 3.07 nm. In our simulations, pure lipid bilayers have an average thickness of 3.05 nm; thus the overall membrane thickness is not altered significantly with a transmembrane protein present.

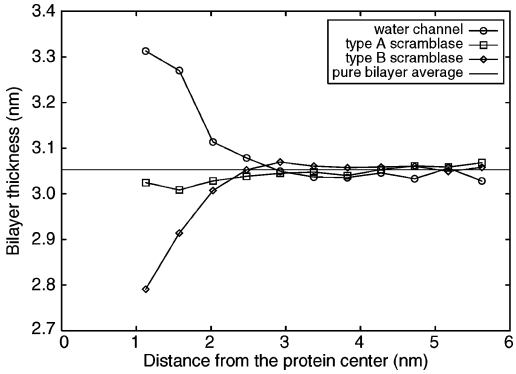

Figure 4. Altered membrane thickness around the transmembrane proteins. The membrane thickness is measured in concentric rings around the transmembrane protein center and averaged over 72 ns. The bilayer thickness depends on the distance to the transmembrane protein.

However, a commonly accepted theory suggests that a height mismatch between the hydrophobic part of a transmembrane protein and the hydrophobic part of a lipid bilayer leads to hydrophobic matching; that is, the transmembrane protein locally imposes its hydrophobic height on the membrane. Because contact between polar and apolar groups is preferably minimized and the lipid phase is much more deformable than a protein, a state of membrane deformation is considered less costly than a state of hydrophobic mismatch. The dimeric β-helical ion channel gramicidin, for instance, has been demonstrated to change membrane thickness.[24] Depending on the rigidity of the lipids, at a certain distance from the protein the membrane thickness returns to normal.

The extent of hydrophobic matching in our system is visualized in Figure 4, for the case of both the water channel and the two scramblases. From the figure, it is clear that close to the water channel the membrane thickness is about 10% larger than the normal thickness of 3.05 nm. The transmembrane protein locally changes the structure of the bilayer. For the type A scramblases, despite the identical base height, the hydrophobic mismatch is lower. This is because the water channel's coating particles can spread between the tetrahedral ends, thereby enlarging its hydrophobic length. The difference between the hydrophobic matching patterns of type A and B scramblases is due to the mobility of the lipid headgroups near the hydrophilic band of type B. Close to the protein the thickness has changed significantly, but in all three cases the difference has vanished at about 2.5 nm from the protein center. Because of the inherent flexibility of the lipids in our model, the affected area is quite small.

3.1.2. Aggregation. Hydrophobic matching putatively drives a membrane-mediated protein−protein attraction. With multiple transmembrane proteins, aggregation is energetically favorable as this reduces the area of the membrane that needs to be deformed. The distance over which this protein attraction functions therefore depends on the rigidity of the bilayer as well. From Figure 4 follows that in this model the protein−protein distance at which the mutual attraction is significant is at most 5 nm.

However, in a simulation with 14 type A scramblases and 144 lipids there is little aggregation of scramblases. Instead, a dynamic equilibrium is established in which the scramblases connect and disconnect regularly (Figure 5a). Upon closer inspection, it follows that the lack of aggregation is due to the shape of the scramblases. The tetrahedral ends prohibit full contact between the scramblases so there is always room for a lipid tail to interfere, thereby negating stable protein−protein

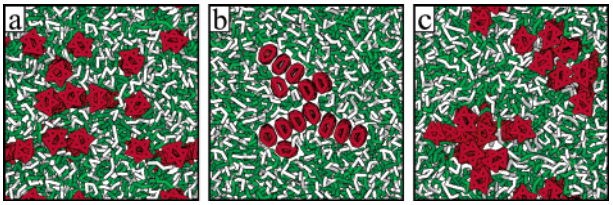

Figure 5. Several modes of aggregation; shown is a top view of the bilayer with 14 transmembrane proteins. (a) Weak aggregation of regular type A scramblases; they connect and disconnect regularly (72 ns). (b) Strong aggregation of type A scramblases trimmed of the tetrahedral parts; none of the proteins dissociate (72 ns). (c) Intermediate aggregation of type B scramblases; two pore complexes are formed (72 ns).

interaction. When the simulation is redone using scramblases without the tetrahedral endgroups (Figure 5b), a different picture emerges, despite the hydrophobic matching being markedly similar. As these proteins can connect tightly across their entire length and through optimal packing have maximal van der Waals attraction, one big aggregate is formed after 15 ns of simulation time. In the remainder of the simulation, none of the proteins dissociate from the aggregate. When type B scramblases are used instead of the hydrophobic ones, the level of aggregation is intermediate (Figure 5c). As the tetrahedral ends inhibit full contact, aggregates are still dynamic, but as the hydrophilic bands are preferentially near each other, there is an extra inclination to aggregate. During the course of this simulation, the type B scramblases cluster with their bands together. Eventually these clusters grow into two large clusters of 7 proteins each, each forming a pore complex in the membrane.

3.1.3. Function. 3.1.3.1. Water Channel. To test the effectiveness of our water channel, W particle permeation rates have been measured and multiplied by 4 to match regular permeation rates. Our coarse-grained water channel thus achieves a rate of 2.7×10^{-15} mol/s. The maximal flow through an aquaporin subunit has been determined to be about 5×10^{-15} mol/s.[25] These rates are comparable, despite the fact that our simulations are performed under steady-state conditions, whereas the aquaporin flow has been determined under forced osmotic pressure.

The permeation rate of water through a pure lipid membrane in our model is 13.9×10^{-5} m/s, which is well within the order of magnitude of the experimental diffusive water permeability of DPPC (5×10^{-5} m/s).[26] Incorporating 1 water channel in a 225 lipid membrane leads to a permeation rate through the membrane as a whole of 43.0×10^{-5} m/s.

3.1.3.2. Scramblase. First, one type A scramblase is tested in a flat lipid bilayer of 225 lipids to see whether it induces flip-flop and by what mechanism. In all our pure lipid bilayer simulations, no spontaneous flip-flop was ever encountered, so any flip-flop due to the scramblase would be of significance. To stimulate flip-flop, a lipid gradient is created by removing 25% of one monolayer's lipids. However, despite the scramblase, in 72 ns not a single lipid flipped, just as in the control simulation without scramblase. Increasing the protein content (as in the aggregation experiment), while maintaining the lipid gradient, yields a membrane of 14 scramblases and 126 lipids, but still no flip-flop occurs. Instead of locally disturbing the lipid continuum, as predicted by Kol et al.,[18] the multitude of type A scramblases stabilizes the bilayer; for instance, the lateral diffusion rate of lipids is reduced by 35%. As the absence of flip-flop might be due to the lack of undulations in the small box, the bilayer length is tripled in one direction. Yet, although this membrane exhibits considerable undulations with large amplitudes, no flip-flop occurs in this simulation as well.

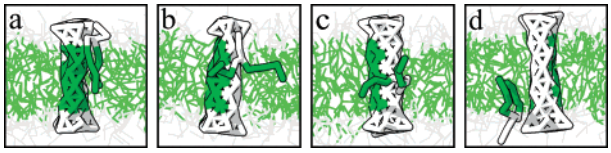

Figure 6. A lipid flips headfirst along a type B scramblase; each frame is 0.24 ns apart.

As none of the hydrophobic scramblases prompted lipid flip-flop, configurations with a hydrophilic band have been tested in the small bilayer as well. These type B scramblases do enhance flip-flop, but as a side effect also allow water to traverse the bilayer; during 72 ns, 14 lipids and 221 water particles traversed the bilayer. Each lipid flip is characterized by movement of the lipid headgroup along the hydrophilic band, while the lipid tail ends remain in the bilayer interior (Figure 6). The lipid can flip headfirst with tails splayed or sideways with tails together. In a full bilayer, without lipid gradient, the scramblase functions a bit slower; 44 lipids flipped and 1672 water particles traversed the bilayer in 720 ns. The water flux (1.54×10^{-14} mol/s) is about 10 times faster than through our coarse-grained water channel, so the scramblase also functions as a water channel. Yet, contrary to the aggregation experiment, with a single scramblase a constant water pore is not formed; the type B scramblase merely allows water particles to slip through the bilayer more frequently. Compared to this single scramblase, the flip-flop capacity of the multiple pore-forming scramblases of the aggregation experiments is reduced. As these scramblases aggregated, and thus work together during flips, their solitary flip-flop capacity has diminished from 6.1×10^{-2} flip/ns/protein in the single scramblase simulation to 1.6×10^{-2} flip/ns/protein.

Whenever flip-flop function is required hereafter, type B scramblase will be used exclusively, whereas type A will be used as a nonfunctional protein in control experiments.

3.2. Small Vesicles. With the effect of the coarse-grained water channel and type B scramblase sufficiently validated in lipid bilayers, the proteins are incorporated in vesicles.

3.2.1. Scramblase in an Isolated Vesicle. To test the effectiveness of one type B scramblase in a vesicle, a lipid gradient has been imposed by placing the vesicle of 255 lipids in a larger water-filled box with another 225 lipids dispersed randomly around it. A portion of these lipids will enter the outer monolayer right from the start, while the rest forms micelles that will, eventually, merge with the outer monolayer. Thus, a skewed lipid distribution is generated, and as a result the outer monolayer becomes stressed.

In the control simulation, the nonfunctional type A scramblase is used. The top graph of Figure 7 depicts the time course of the lipid ratio between exterior and interior lipids, and the absolute number of interior lipids and water particles. The number of interior molecules increases stepwise twice. Each step is the result of a novel vesicle enlargement process we will refer to as the engulfing lobe.

As the outer monolayer cannot pass on lipids to the inner monolayer, it cannot take in more lipids while maintaining a normal flat structure. Instead, once the uptake limit is reached, additional micelles become part of the outer monolayer and are not fully absorbed but form a bilayerlike attachment (Figure 8a). Lipids from the tense outer monolayer allow this lobe to grow larger, as it proceeds to curl into a semi-vesicle (Figure 8b). Before the lobe becomes another vesicle on top of the initial one, a pore opens at its base, allowing enveloped water particles and lipids to enter the initial vesicle (Figure 8c,d). Thus, the

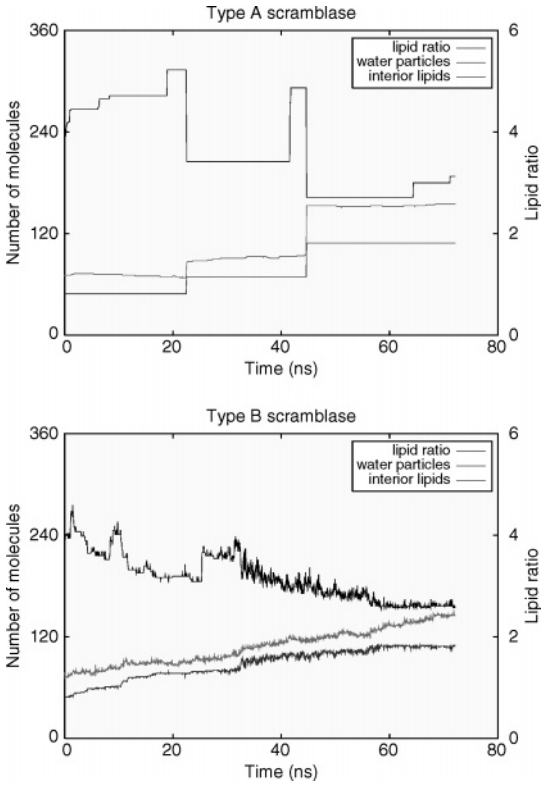

Figure 7. The vesicular contents and lipid ratios followed through time as additional lipids are incorporated in a small vesicle with type A scramblase (top) and type B scramblase (bottom).

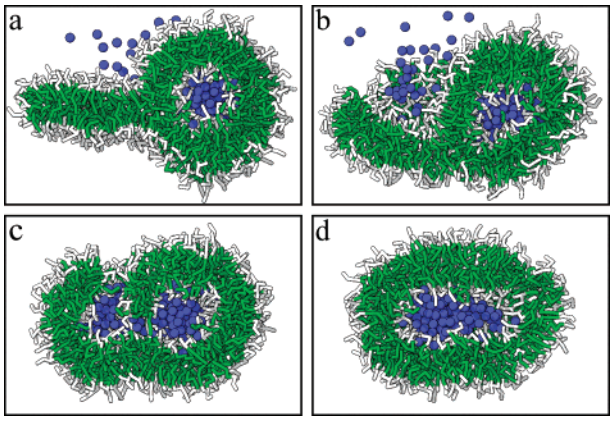

Figure 8. The engulfing lobe process demonstrated in a small vesicle that takes up additional lipids. (a) A micelle merges with the outer membrane (42.4 ns). (b) The micelle bends (43.6 ns), (c) and a transient pore emerges at its base (44.6 ns). (d) The vesicle after it has taken up lipids and water (46.6 ns).

engulfing lobe mechanism is a spontaneous vesicle enlargement mechanism whereby the vesicle uses surplus exterior lipids to take up a portion of these lipids and additional water.

Over the course of this simulation, all exterior lipids became part of the vesicle; each added lipid raised the lipid ratio and the membrane tension. The first lobe emerged and engulfed water in 3.4 ns at a lipid ratio of 5.1:1; the second lobe cycle took 3.0 ns at a ratio of 4.8:1. At the end of the simulation, the vesicle is elongated and its lipid ratio is 3.1:1.

When the simulation is redone with a type B scramblase, a different growth pattern develops (Figure 7, bottom). The banded scramblase quickly redistributes the lipids that merge with the outer monolayer. Hence, the number of interior lipids and water particles increase steadily, while the lipid ratio decreases steadily. This vesicle does eventually adopt a spherical shape.

TABLE 1: Overview of Vesicle Fusion Simulations Performed[a]

label	N_{out}	N_{in}	N_W	fusion pathway	N_{out}/N_{in}
PURE1	134	26	17	anisotropic, 1 pore	3.78
PURE2	161	39	66	anisotropic, 2 pores	3.40
PURE3	181	58	102	radial	3.12
PURE4	655	369	3483	anisotropic, 1 pore	1.68
PURE5	655	369	3497	anisotropic, 2 pores	1.70
SCRB1	176	49	70	anisotropic, scramblase pore	2.98
SCRB2	638	380	3555	anisotropic, scramblase pore	1.65
WACHA1	180	45	85	anisotropic, 2 pores	3.59
WACHA2	180	45	92	radial	4.00

[a] The simulations are labeled PURE for vesicles consisting only of lipids, SCRB for vesicles with type B scramblases, and WACHA for vesicles with water channels. For these simulations, the number of lipids in the inner (N_{in}) and outer (N_{out}) membrane layer of each vesicle, the number of encapsulated water particles (N_W) in each vesicle, the fusion pathways, and the lipid distribution ratio of the vesicle membrane (N_{out}/N_{in}) are given. The lipid distribution is calculated immediately after the development of a hemifusion diaphragm or a double pore.

3.3. Small Vesicle Fusion. In the following sections, several vesicle fusion simulations are discussed; their characteristics are summarized in Table 1. First, small vesicles are fused, because by utilizing small vesicles we can relatively quickly determine the effect of the various proteins on the vesicles during and after fusion. Subsequently these simulations are verified with larger vesicles.

3.3.1. Pure Lipid Vesicle Fusion. We previously demonstrated that our model exhibits spontaneous vesicle fusion processes that conform to literature predictions, including stalk formation, radial or anisotropic expansion to the hemifusion diaphragm (HD) state, and subsequent degradation of the HD to full fusion.[1] In the radial stalk expansion process, the stalk spreads out so the inner monolayers come into contact, thus forming an HD. In the anisotropic stalk−pore process,[27] the stalk elongates in the contact zone and bends to form a ring. Before the ring becomes complete, either one or two transient pores emerge in its center. When two pores are present, the vesicles are fused instantly. When one is present, it allows the pocket in the ring to be internalized into the vesicle, whereby an HD is formed. Once another pore emerges in the HD, full fusion is reached. In the present study, these plain vesicle fusion simulations serve as control experiments, labeled PURE1−5.

3.3.2. Vesicle Fusion with Water Channels. As mentioned in the Introduction, a vesicle's shape is preferentially spherical, yet the resultant vesicles of pure lipid vesicle fusion simulations remain tubular throughout the simulations. Provided that the required membrane tension and water permeability are present, water can simply diffuse through the membrane to increase vesicle volume and thus create a spherical vesicle. Here, we test the hypothesis that increased water permeability, due to the presence of a water channel, enables fused vesicles to become spherical faster.

In this simulation (WACHA1), each vesicle consists of 225 lipids and 1 water channel. Full fusion is reached through the anisotropic stalk expansion pathway, here followed by double pore formation after 4.0 ns. This fast fusion is similar to the fusion of regular small vesicles (PURE1, PURE2). The result is quite similar as well; the vesicle remains tubular and there is no significant increase in volume apart from the uptake during the stalk-bending part of fusion. The effect of the water channels is simply that the water content fluctuates more. Apparently, in their current configuration there is not enough incentive for the vesicles to become spherical.

In this case, aggregation of water channels is significant. Compared to the flat bilayer case, the vesicle's bilayer has a different structure; this causes a larger hydrophobic mismatch, thus increasing the cost of membrane deformation and the strength of aggregation. After 17.8 ns, the inner ends of the water channels make contact, the outer ends 3.0 ns later, and then the last of the intervening lipids departs. For most of the remainder of this simulation, the two water channels remain attached to each other, yet this attachment is by no means fixed. For several short intervals, ranging from 60 ps to a few nanoseconds, the inner or outer ends dissociate.

In a second simulation involving these vesicles, but with a slightly different initial configuration (WACHA2), the outcome is quite different. The stalk initially grows anisotropically, but reverts to expand radially. This series of events is analogous to a simulation performed with pure vesicles (PURE3). Because of this fusion pathway, the membrane lipid distribution and water content of the resultant vesicle are identical to (the sum of) those of the vesicles before fusion. Therefore, the vesicle has little water content situated in a thin cylinder of hydrophilic particles, and the outer monolayer experiences more tension than in WACHA1. This structure changes into a spherical vesicle with a large lobe, thereby maximizing hydrophilic interactions and relieving membrane tension. The vesicle proceeds to take up water and lipids through the engulfing lobe process. As the water channels are not involved in the lobe's appearance, this simulation suggests the engulfing lobe's applicability in regular vesicle fusion. Despite the improvement in lipid and water distribution made by the engulfing lobe, the vesicle remains tubular in shape. Again, the water channels aggregate.

3.3.3. Vesicle Fusion with Type B Scramblases. Even though MD simulations of vesicle fusion do not produce spherical vesicles, Brownian dynamics simulations have shown this behavior.[28] However, those vesicles have properties inconsistent with naturally occurring vesicles. Spontaneous swelling occurs because their solvent is represented by a potential acting on the lipids rather than by explicit solvent particles. Moreover, the lipids are able to spontaneously exchange between the monolayers. As increased water permeability is insufficient to ensure spherical vesicles in our MD simulations, we hypothesize that frequent flip-flop of lipids is also required.

With the scrambling effect of type B scramblase demonstrated in bilayers and vesicles, we next test whether it actually allows small fusing vesicles (SCRB1) to become spherical. Furthermore, these simulations suggest that scramblase can facilitate fusion via the anisotropic stalk expansion as well. The scramblase, which happens to be near the stalk region, allows the formation of a pore along its hydrophilic band (Figure 9a). During the 1.2 ns that the pore lasts, 9 lipids and 30 water particles enter the vesicle. The lipid transfer is in the same order as in comparable simulations that exhibit the anisotropic stalk−pore process (PURE1, PURE2), whereas the water transport is roughly doubled. A hemifusion diaphragm is already present before pore closure (Figure 9b); the pore is part of the vesicle wall. The pore closes and another pore opens in the HD immediately thereafter (Figure 9c). In this manner, fusion is

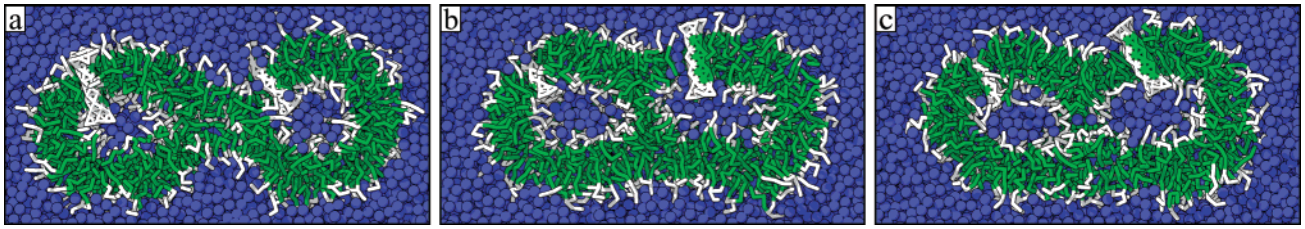

Figure 9. Cross-sectional view of the stalk−pore transition facilitated by a type B scramblase. (a) While the stalk is expanding anisotropically, a pore is formed next to the hydrophilic band of the scramblase in the vesicle on the right (3.2 ns). (b) A hemifusion diaphragm is already present, while the pore is still open (4.3 ns). (c) When the pore closes, another pore opens in the HD, completing the fusion process (4.4 ns).

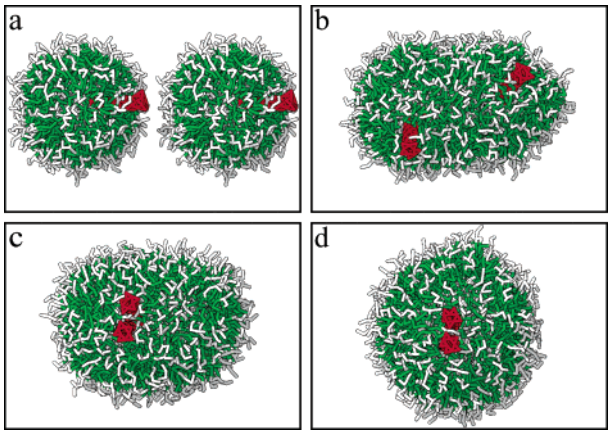

Figure 10. The fused vesicle becomes spherical when type B scramblases are present. (a) The initial setup (0 ns). (b) After fusion, the resultant vesicle is still elongated (21.6 ns). (c) When the scramblases find each other, they aggregate (91.4 ns). (d) Despite aggregation, the scramblases remain to function, and consequently the vesicle becomes spherical (336 ns).

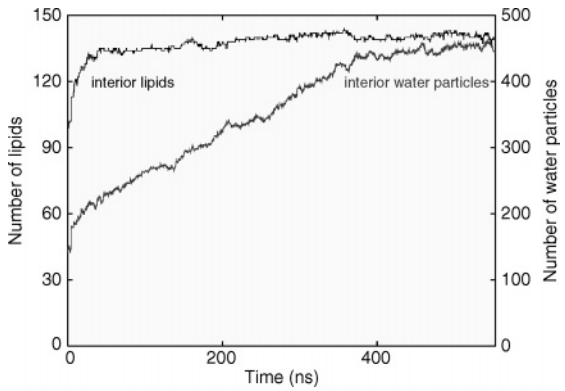

Figure 11. The development of the number of interior lipid molecules and water particles following vesicle fusion. The lipid content reaches a plateau well before the water content does.

reached by the same lipid and water dynamics as present in anisotropic stalk−pore process, but the pore is induced by the amphiphilic peptide.

As the vesicles are fully fused within 4.4 ns, the bulk of the simulation time is spent on adaptation of the vesicle (Figure 10). Figure 11 shows the time course of the contents of the vesicle. In this case, the time for equilibration is roughly 100 times as long as the time for fusion. Evidently, the number of internal lipids increases rapidly the first 35 ns and changes only marginally thereafter. The water content increases very fast during the fusion process and steadily thereafter, until about 325 ns, when the vesicle reaches an equilibrium state. The shape of the vesicle can be deduced from the graphs depicting the three principal diameters versus time (Figure 12). A perfect sphere would show three superimposed lines, but this result is not expected. A vesicle with a type B scramblase equilibrates

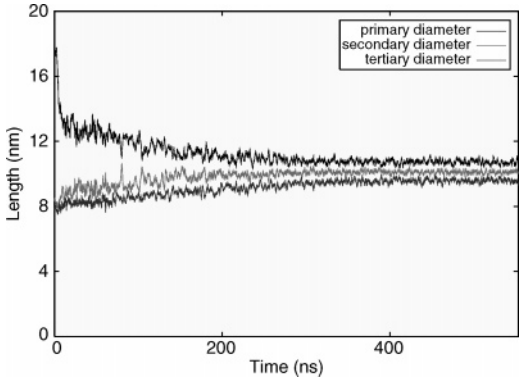

Figure 12. The "primary", "secondary", and "tertiary diameter" computed with principal component analysis and smoothed with a moving average window of 1 ns. As the lines converge, the vesicle becomes spherical.

by releasing excess membrane tension. Without tension, the membrane will be able to undulate and thus does not have the shape of a perfect sphere. Nevertheless, the graph shows that the fused vesicle becomes rather spherical.

Apparently, the lipids are faster than water at adapting to the new situation. However, the fact that the vesicle is not spherical in the early stages does not mean that the lipid distribution corresponding to a spherical vesicle is unfavorable; the lipids move from the regions of high membrane tension regardless of the overall shape of the vesicle. Nonetheless, for the vesicle to become spherical, and for the system to gain another level of energy minimization, water has to diffuse into the vesicle. This diffusion is rate limiting as the steady increase in water content shows.

The final vesicle has 140 lipids and 446 water particles inside and 310 exterior lipids. Of those 446 water particles, only 9 were initially present in the vesicles. This shows that there is much water exchange; even though the banded scramblases do not form actual water pores as seen in the aggregation experiment, they vastly increase membrane permeability. The scramblases do aggregate, and after 51 ns they connect and remain so for the rest of the simulation.

3.4. Fusion of Large Vesicles. To see whether the effects of type B scramblase in small vesicle fusion can be reproduced in large vesicles, we perform such a simulation as well. The simulation (SCRB2) consists of two large vesicles of 1018 lipids and 4 type B scramblases each. Similar to prior large vesicle fusion simulations (PURE4−5), fusion starts by following the anisotropic stalk expansion pathway. Again, the scramblase facilitates fusion; a pore is initiated by a scramblase that happens to be in the center of the stalk ring. Through the pore, 13 lipids and 27 water particles enter the vesicle. With the formation of an HD, the pore closes. As no pore is formed in the HD in the short time after HD formation, the equilibrating properties of the banded scramblases stabilize this hemifusion state. The graphs of Figure 13 show that the vesicle labeled B is the one

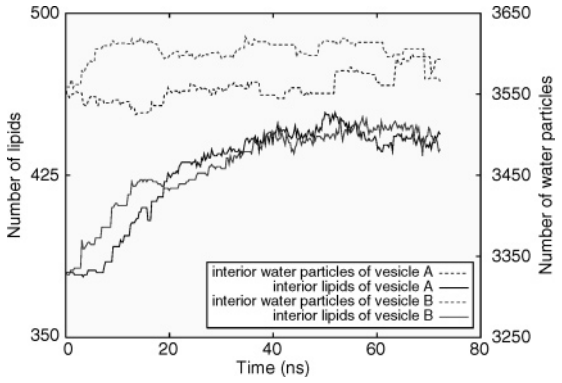

Figure 13. Development of the number of interior lipid molecules and water particles of the large vesicles of SCRB2. Their contents remain separated for the entire simulation.

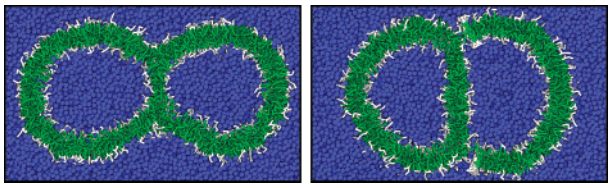

Figure 14. Cross-sections of the hemifusion diaphragm states of PURE4 (left) and SCRB2 (right). Whereas the hemifusion state in PURE4 has a characteristic hourglass shape and a thin HD as compared to the outer membrane, the type B scramblases − here two of them are shown lying to the right of the HD − have equilibrated the HD state in SCRB2. Consequently, the whole membrane of SCRB2 has obtained a uniform thickness, and the hourglass shape is gone.

where the pore has formed. However, the scramblases proceed to equilibrate the vesicles so that earlier on the lipid content, and later also the water content, becomes similar for both vesicles. Compared to PURE4, the vesicle loses its hourglass shape and the diaphragm grows into a stable bilayer as thick as the outer membrane (Figure 14). Therefore, a destabilizing pore in the HD is not likely to appear.

With multiple type B scramblases, a certain level of aggregation, maybe even peptide pore formation, is anticipated. However, only 2 out of 8 scramblases have actually aggregated in the 72 ns the simulation lasted. Nonetheless, the interaction of the peptides with the membrane does stimulate the scramblases to move toward the HD. All but one of the scramblases settle in this region, with their hydrophilic bands turned toward the HD.

3.5. Bilayer Fusion. Giant vesicles are not able to fully fuse without an extra driving force,[29] thus various fusion protein models were conceived.[6] As an MD simulation of giant vesicle fusion is as yet unfeasible in both the length and the time scale accessible by the currently available fastest computers, we focus on the contact zone. At such a scale the vesicle membrane appears flat, so a representative simulation contains two bilayers with a small water layer in between. Like in in vitro experiments,[30] two flat bilayers do not fuse spontaneously in our simulations.[1] However, when the bilayers are placed sufficiently close together so they are able to undulate into contact range, a stalk is formed. This stalk then grows anisotropically into one large elongated stalk; it bends depending on the local shape of the contact zone, but not into a small ring. This hemifusion state is stable, and a hemifusion diaphragm state is not reached.

Here, we test whether addition of type B scramblases permits two flat membranes to fuse. Our simulation setup consists of two parallel bilayers containing 890 and 899 lipids and 2 type B scramblases each; the adjacent monolayers are separated by an average of 3.4 layers of water particles, the distant monolayers by 12.4 layers. During stalk elongation, all four scramblases end up next to the stalk, but they do not aggregate. As the stalk keeps on growing, it meanders around the scramblases. Moreover, the scramblases in the opposite bilayers form pairs. In effect, the scramblases are linked together at the ends, as they both favor to be next to the bent stalk. The pairs subsequently allow formation of a continuous water pore (Figure 15). When the bilayers are regarded as the contact zone of giant vesicles, these pores allow the vesicles' content and inner monolayers to mix. Thus, this state corresponds to full fusion facilitated by two pairs of banded scramblases.

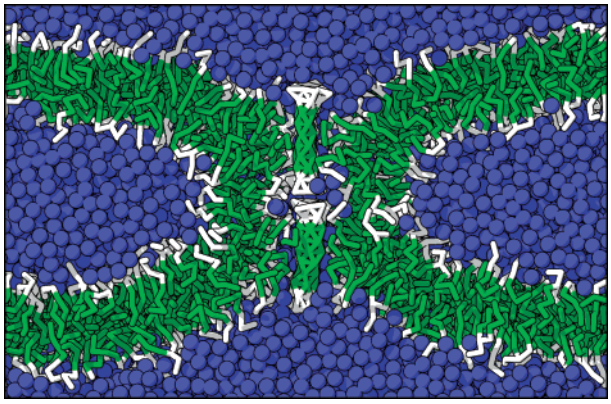

Figure 15. Cross-sectional side view of two fused horizontal bilayers. A fusion pore has been established by two paired type B scramblases.

4. Discussion

4.1. Hydrophobic Matching and Aggregation. In our simulations, we have verified the existence of changed membrane thickness due to hydrophobic matching of lipid bilayers to transmembrane proteins. On the basis of the structural differences between bilayers and vesicles, the latter having a reduced membrane thickness among other things, it is probable that the mismatch is larger in case of a vesicle. As the fused vesicle in the WACHA1 simulation did not become spherical, there are areas of minimal curvature. Indeed, the water channels stay in the areas where hydrophobic mismatch is minimal, in this case, areas that resemble a bilayer the most. Therefore, the water channels favor the side of the tubular vesicle as opposed to the rounded ends. In fact, they even pair along the length axis of the vesicle where curvature is minimal. A similar kind of preference is exhibited by the type B scramblases in SCRB2; they group around the hemifusion diaphragm. In the aggregation simulation with multiple scramblases, the level of transmembrane peptide aggregation was shown to be strongly dependent on complementing contact shapes and hydrophobicity.

In the simulations presented here, and in the simulations of others,[31,32] the addition of a transmembrane peptide locally altered the membrane thickness. However, the experimental addition of an isolated WALP helix into bilayers did not alter membrane thickness.[33] This was attributed to an assumed difference in packing of lipids around a single transmembrane helix as compared to a large protein. The reason for this disagreement in results may be that the membrane thickness is altered only slightly and locally, comparable to our 1.5% decrease in 2.5 nm around the protein center, which is difficult to detect experimentally.

4.2. Engulfing Lobe. The engulfing lobe, a novel spontaneous vesicle enlargement process, was observed in the small vesicle simulations. What are the prerequisites for a vesicle to enlarge via an engulfing lobe, and could it be universally present in nature? The most obvious requirement is that the outer mono-

layer is made up of enough lipids to cover the inner monolayer and simultaneously form a substantial bilayer appendage. In addition, the outer monolayer must be under considerable tension due to crowdedness. Of course, the effective lipid shape is important in lobe formation as well as in lobe curvature. The first two requirements are typically only met in small vesicles after fusion. In MD simulations,[1,34] vesicles were spontaneously generated with a lipid content of 150 and up. Such tiny vesicles are not easily found in the in vitro experiments; we expect they rapidly fuse into larger ones.

The engulfing lobe process might be an additional mechanism for fast flip-flop in biogenic membranes. The reason protein involvement is implied is essentially that, in vitro, lipids do not spontaneously flip frequently. However, this flip-flop activity is measured under steady-state conditions in stable membranes, whereas the biogenic membrane is characterized by growth of a single monolayer and as such inherently unstable. In the simulation of the vesicle with additional lipids, such a condition is quickly resolved by the appearance of multiple engulfing lobes.

4.3. Scramblase Flip-Flop. At first glance, the hypothesis that the mere presence of transmembrane proteins causes substantial lipid flip-flop[4,18] is not readily supported by our simulations. One of the principles the hypothesis conveys is that transmembrane helices in bilayers produce sufficient disorder for the lipid headgroups to slip into the bilayer, and subsequently pop-up on the other side. Our simulations show little disorder near the type A scramblases. However, the different outcomes of the in vitro and in silico experiments might simply be due to the different time scales at which they are measured. The flip-flop rate of the in vitro experiments is much lower than the perceived rate in the simulations with the type B scramblases. With certainty, the flip-flop effect of type A scramblases cannot be rejected, for the bilayer simulations might just have to be extended for the effect to show.

On the other hand, the experimental lipid flips might be linked to a dynamic equilibrium of transmembrane helix insertion and expulsion, instead of helices that are stable in a bilayer. The latter is at least suggested by MD simulations of transmembrane peptide insertion,[12] where insertion is accompanied by transbilayer movement of lipids chaperoning the hydrophilic ends. The "barrel-stave" mechanism[23] is another putative bilayer insertion mechanism for amphiphilic transmembrane helices resembling the type B scramblases. It states that multiple peptides drift over the surface of the membrane, but upon aggregation fold into the membrane together, thus forming an instant hydrophilic pore, which subsequently allows water permeation and lipid flip-flop. We have shown that with multiple amphiphilic helices such pore formation does occur, but aggregation is not quite necessary for an increase in the water permeability and flip-flop rate.

4.4. Fusion Facilitated by Type B Scramblases. Apart from enhancing spontaneous flip-flop, type B scramblase has been demonstrated to promote fusion as well. It does so by providing a way to relieve membrane tension that results from crowding of the outer monolayer due to growth of the stalk. Normally, the tension rises until it is relieved by a pore appearing in the stalk ring; here the hydrophilic band promotes pore formation. In essence, this is still the result of changing the rates of flip-flop and water permeation. This may explain the results of Müller et al.[35] Using Monte Carlo simulations of block copolymers, they found full fusion of two bilayers, something which is not normally found in natural bilayers or MD simulations. However, compared to lipid bilayers, their membranes already have increased flip-flop and water permeation rates. The major difference between their model and our lipid bilayers including scramblase is that, like proteins, the scramblase functions locally; its rate of lipid flip-flop depends on the local gradient. For example, in the SCRB1 simulation, the banded scramblase that formed the pore allowed 9 lipids to enter the vesicle, and the other let only 2 lipids in. In this simulation, the time from stalk to HD was decreased compared to the equivalent simulations PURE1−2, but not by many orders of magnitude (from 2.91, 2.02, to 1.66 ns). However, the fact that banded scramblases can induce a pore next to a stalk means that much larger vesicles and bilayers are also able to fuse. In this sense, the scramblase functions as a fusion protein. Of the various putative fusion protein models that permit flat membranes to fuse,[6] the local perturbation model and the proteinaceous fusion pore model both describe the shape and characteristics of type B scramblase well. The first model is loosely defined; it merely features leaky fusion induced by amphiphilic peptides that are said to disturb the membrane. The second model suggests that multiple amphiphilic transmembrane peptides form pore complexes in both fusing membranes. The complexes of opposing membranes connect, and subsequently the pore subunits dissociate to let the lipids unite the opposing bilayers. Although the type B scramblases can form such an instant pore by aggregation, in the simulation of bilayer fusion, the fusion pore was not of this nature. Association of opposing scramblases did occur, and a fusion pore has been established, but guided by an elongated stalk. Thus, our simulations suggest an alternative proteinaceous fusion pore model with a larger role for lipid dynamics.

5. Conclusion

With our coarse-grained molecular dynamics model previously, only lipid interactions were simulated; in this paper, we have demonstrated its use in simulations involving protein−lipid interactions. We introduced model proteins that enhance the bilayer's ability for water permeability and lipid flip-flop. When incorporated in membranes, these transmembrane proteins induced hydrophobic matching of the membrane and accordingly protein aggregation was present. The strength of aggregation depends on the fit of the proteins. In some of the simulations, a novel vesicle enlargement process, referred to as the engulfing lobe, was observed. This mechanism might have gone unnoticed experimentally, due to its rapid development on a small membrane area.

Although inclusion of a water channel increased water flow through the membrane, the fused vesicle did not become spherical; the lipid distribution of the membrane needed to adapt as well. To test the hypothesis that protein presence in general promotes fast flip-flop, model transmembrane helices were incorporated in various bilayers and vesicles, but without result. Pore-forming antimicrobial peptides are known to combine pore-formation and flip-flop. The current view is that fully developed proteinaceous pores are needed to promote flip-flop. Using a coarse-grained equivalent, our simulations show that for both increased water transport and lipid flip-flop a single peptide is sufficient, although multiple peptides do aggregate into pore complexes. This peptide was found to equilibrate fused vesicles, which subsequently became spherical, and also to accelerate and even enable fusion in systems that normally do not fully fuse.

References and Notes

(1) Smeijers, A. F.; Markvoort, A. J.; Pieterse, K.; Hilbers, P. A. J. *J. Phys. Chem. B*, **2006**, *110*, 13212−13219.

(2) Marrink, S. J.; Mark, A. E. *J. Am. Chem. Soc.* **2003**, *125*, 11144−11145.
(3) Stevens, M. J.; Hoh, J. H.; Woolf, T. B. *Phys. Rev. Lett.* **2003**, *91*, 188102.
(4) Kol, M. A.; de Kroon, A. I. P. M.; Rijkers, D. T. S.; Killian, J. A.; de Kruijff, B. *Biochemistry* **2001**, *40*, 10500−10506.
(5) Matsuzaki, K.; Murase, O.; Fujii, N.; Miyajima, K. *Biochemistry* **1996**, *35*, 5, 11361−11368.
(6) Jahn, R.; Grubmüller, H. *Curr. Opin. Cell Biol.* **2002**, *14*, 488−495.
(7) Markvoort, A. J.; Pieterse, K.; Steijaart, M. N.; Spijker, P.; Hilbers, P. A. J. *J. Phys. Chem. B* **2005**, *109*, 22649−22654.
(8) Sui, H.; Han, B. G.; Lee, J. K.; Walian, P.; Jap, B. K. *Nature* **2001**, *414*, 872−878.
(9) Nielsen, S. O.; Lopez, C. F.; Srinivas, G.; Klein, M. L. *J. Phys.: Condens. Matter* **2004**, *16*, R481−R512.
(10) Fujiyoshi, Y.; Mitsuoka, K.; de Groot, B. L.; Philippsen, A.; Grubmüller, H.; Agre, P.; Engel, A. *Curr. Opin. Struct. Biol.* **2002**, *12*, 509−515.
(11) Tajkhorshid, E.; Nollert, P.; Jensen, M. Ø.; Miercke, L. J. W.; O'Connell, J.; Stroud, R. M.; Schulten, K. *Science* **2002**, *296*, 525−530.
(12) Lopez, C. F.; Nielsen, S. O.; Ensing, B.; Moore, P. B.; Klein, M. L. *Biophys. J.* **2005**, *88*, 3083−3094.
(13) Hummer, G.; Rasalah, J. C.; Noworyta, J. P. *Nature* **2001**, *414*, 188−190.
(14) Sasaki, Y.; Shukla, R.; Smith, B. D. *Org. Biomol. Chem.* **2004**, *2*, 214−219.
(15) Tannert, A.; Pohl, A.; Pomorski, T.; Herrmann, A. *Int. J. Antimicrob. Agents* **2003**, *22*, 177−187.
(16) Alberts, B.; Bray, D.; Lewis, J.; Raff, M.; Roberts, K.; Watson, J. D. *Molecular Biology of the Cell*; Garland: New York, 1994.
(17) Daleke, D. L. *J. Lipid Res.* **2003**, *44*, 233−242.
(18) Kol, M. A.; de Kroon, A. I. P. M.; Killian, J. A.; de Kruijff, B. *Biochemistry* **2004**, *43*, 2673−2681.
(19) Marx, U.; Lassmann, G.; Holzhütter, H. G.; Wüstner, D.; Müller, P.; Höhlig, A.; Kubelt, J.; Herrmann, A. *Biophys. J.* **2000**, *78*, 2628−2640.
(20) Kol, M. A.; van Dalen, A.; de Kroon, A. I. P. M.; de Kruijff, B. *J. Biol. Chem.* **2003**, *278*, 24586−24593.
(21) Menon, A. K.; Watkins, W. E., III; Hrafnsdóttir, S. *Curr. Biol.* **2000**, *10*, 241−252.
(22) Nomura, K.; Corzo, G.; Nakajima, T.; Iwashita, T. *Biophys. J.* **2004**, *87*, 2497−2507.
(23) Shai, Y. *Biochim. Biophys. Acta* **1999**, *1462*, 55−70.
(24) Harroun, T. A.; Heller, W. T.; Weiss, T. M.; Yang, L.; Huang, H. W. *Biophys. J.* **1999**, *76*, 937−945.
(25) Zeidel, M. L.; Ambudkar, S. V.; Smith, B. L.; Agre, P. *Biochemistry* **1992**, *31*, 7436−7440.
(26) Garrett, R. H.; Grisham, C. M. *Biochemistry*; Saunders College Publishing: Fort Worth, TX, 1995.
(27) Kozlovsky, Y.; Chernomordik, L. V.; Kozlov, M. M. *Biophys. J.* **2002**, *83*, 2634−2651.
(28) Noguchi, H.; Takasu, M. *J. Chem. Phys.* **2001**, *115*, 9547−9551.
(29) Heuvingh, J.; Pincet, F.; Cribier, S. *Eur. Phys. J. E* **2004**, *14*, 269−276.
(30) Yang, L.; Huang, H. W. *Science* **2002**, *297*, 1877−1879.
(31) Petrache, H. I.; Zuckerman, D. M.; Sachs, J. N.; Killian, J. A.; Koeppe, R. E., II; Woolf, T. B. *Langmuir* **2002**, *18*, 1340−1351.
(32) Nielsen, S. O.; Ensing, B.; Ortiz, V.; Moore, P. B.; Klein, M. L. *Biophys. J.* **2005**, *88*, 3822−3828.
(33) Weiss, T. M.; Wel, P. C. A.; Killian, J. A.; Koeppe, R. E., II; Huang, H. W. *Biophys. J.* **2003**, *84*, 379−385.
(34) Marrink, S. J.; Mark, A. E. *J. Am. Chem. Soc.* **2003**, *125*, 15233−15242.
(35) Müller, M.; Katsov, K.; Schick, M. *Biophys. J.* **2003**, *85*, 1611−1623.